Supplementary information

Magnetic ordering in $SrMn_{0.925}Sb_{0.075}O_3$

The magnetic structure determination for $SrMn_{0.925}Sb_{0.075}O_3$ was performed from NPD data at 1.5 K and 80 K. An analysis of profile fits after refinement of the nuclear structure showed extra intensities for (11-1) at $d \approx 4.47$ Å and (11-2) at $d \approx 3.88$ Å (Fig. 8).

These reflections of magnetic origin can be indexed with a magnetic cell of the same dimensions and space group as the structural one, which means that we need the single propagation vector k = (0, 0, 0). The magnetic symmetry analysis was performed with the program BasIreps in the FullProf suite [30]. Besides producing the irreducible representations (IRREPs) of the magnetic structure for space group *C*2/*c* and k = (0, 0, 0) (Table S5), the program also calculates the general expressions of the Fourier coefficients $S_k(j)$ of the atoms not related by lattice translations for different sites, in our case the 4*a* and 8*f* sites occupied by magnetic manganese ions with fractions 0.775 and 1.0, respectively (Table S6). There are two IRREPs corresponding to the long-range magnetic ordering of these two magnetic subsystems, Γ_1 and Γ_3, while the other two, Γ_2 and Γ_4, invert the magnetic moment of manganese in site 4*a* and make it paramagnetic. For each of the two sites we need three components of the magnetic moment and only their directions would be changed when going from one atom to the other. There are 12 manganese atoms in the unit cell and six of them (presented in Table S6) are related to six others by a lattice translation t = (½, ½, 0). For the single propagation vector k = (0, 0, 0), according to $m_j = \Psi_j e^{-i2\pi\mathbf{k}\cdot\mathbf{t}}$, where m_j is the magnetic moment at the atomic site *j* in unit cell, Ψ_j is the magnetic moment in the same atomic site in the zeroth unit cell and ***t*** is the translation from one unit cell to another, one has exp(-$i2\pi$**k t**) = exp(0) = 1 [31]. This means that there is no time-reversal operation and magnetic moments after translation would not flip. Two models were constructed with starting magnetic moment equal to $3\mu_B$ for each site and directions constrained according to both IRREPs. The refinement showed that the Γ_1 model perfectly describes the extra intensities (Fig. 8), while the Γ_3 does not at all. But some instability of the refinement process for the Γ_1 model, along with very large estimated errors for m_x and m_y, indicate correlations. Since this structure has just a minor monoclinic distortion compared to the 6*H*-perovskite structure and directions of the magnetic moments are very similar in both structures, the similar symmetry analysis was performed for the parent 6*H*-perovskite structure. The general expressions of the Fourier coefficients $S_k(j)$ of the atoms not related by lattice translations for sites 2*a* and 4*f* in space group $P6_3/mmc$ are presented in Table S7. Since the IRREP Γ_1 of the monoclinic model is similar to Γ_9 of the hexagonal model, the refinement was repeated with m_x and m_y fixed to 0. The quality of fit and R-factors were found to be absolutely the same as those with m_x and m_y unfixed. The relations between the cells and the arrangement of magnetic moments in monoclinic and parent hexagonal lattices are shown in Fig. 3; the difference in fit of NPD pattern of $SrMn_{0.925}Sb_{0.075}O_3$ at 1.5 K without taking into account the magnetic ordering and with long-range magnetic ordering is presented in Fig. 8. In general, Fourier coefficients are (u,v,w) and (-u,v,-w)

and both magnetic subsystems might have antiferromagnetic spin canting in the direction of the *a* axis and ferromagnetic in the direction of the *b* axis, which means that spins are slightly tilted rather than being parallel, and a nonzero net moment is possible. In first approximation, the magnetic structure is well described as A-type antiferromagnetic, where spins are parallel to the *c* axis. In-plane, the coupling is ferromagnetic, while inter-plane the coupling is antiferromagnetic (Fig. 3b). The refined magnetic moments for $SrMn_{0.925}Sb_{0.075}O_3$ at 1.5 K and 80 K are presented in Table S8. The magnitude of the saturated moments at 1.5 K, 1.85(9)μ_B for 4*a* and 1.13(6)μ_B for 8*f* sites, respectively, is much lower than the predicted value of 2.6μ_B for Mn^{4+} with a degree of covalency [32]. The combined populations on both sites of 92.5 % of *S*=3/2 Mn^{4+} and 7.5 % of *S*=2 Mn^{3+} ions mainly leads to antiferromagnetic interactions, although local orbital ordering of Mn^{3+} could create some ferromagnetic couplings causing frustration. Similar long-range magnetic ordering has been reported for the 9*R*-type perovskite, $BaRu_{0.2}Mn_{0.8}O_3$ [33] and hematite, α-Fe_2O_3 [34], below the Morin temperature. More recently, the same magnetic ordering has been published for undistorted 6H perovskite $Ba_3Fe_2TeO_9$ [35].

Magnetic ordering in $SrMn_{1-x}Sb_xO_3$ (x = 0.20, 0.335)

The magnetic structure determination was performed from NPD data of $SrMn_{1-x}Sb_xO_3$ (x = 0.20, 0.335) collected at 5 K. An analysis of fit profiles after refinement of the nuclear structure showed extra intensities for (100) at $d \approx 5.403$ Å, (012) at $d \approx 3.188$ Å, (120) at $d \approx 2.416$ Å and (122) at $d \approx 2.061$ Å (Fig. 10). These reflections can be indexed with a magnetic cell of the same dimensions as the structural one, but the crystallographic unit cell is I-centered, whereas the magnetic unit cell is primitive, which means that we need the single propagation vector k = (1, 0, 0). The magnetic symmetry analysis was performed similarly to the one described above. For space group *I*4/*mcm*, k = (1, 0, 0) and the 4*c* site occupied by magnetic manganese ions with fractions 0.8 and 0.667 for x = 0.20, 0.335, respectively, there are three IREPs, Γ_1, Γ_7 and Γ_{10}, corresponding to magnetic ordering. The general expressions of the Fourier coefficients $S_k(j)$ of the atoms not related by lattice translations are summarized in Table S9. There are 4 manganese atoms in the unit cell and two of them are related to the other two by a lattice translation t = (½, ½, ½). For k = (1, 0, 0), one has $\exp(-i2\pi\mathbf{k}\,\mathbf{t}) = \exp(-i\pi) = -1$ [31], which means that there is a time reversal operation following the translation and that magnetic moments after translation would flip. Three models were constructed with starting magnetic moments equal 3μ_B and directions constrained according to the Γ_1, Γ_7 and Γ_{10} IRREPs The refinement showed that the Γ_7 model perfectly describes the extra peaks (Fig. 10c). The magnetic structure is described as C-type antiferromagnetic, where spins are parallel to the *c* axis with antiferromagnetic intraplanar and ferromagnetic interplanar coupling (Fig. 5b). The refined saturated magnetic moments at 5 K, 2.79(2)μ_B and 2.00(4)μ_B for $SrMn_{1-x}Sb_xO_3$ with x = 0.20 and 0.335, respectively (Table S10), fit well to the predicted value for Mn^{4+}, but are lower than those for Mn^{3+}.

Figure S1. HAADF-STEM images of $SrMn_{0.925}Sb_{0.075}O_3$ taken along the (100) direction. The simulated HAADF-STEM image shown in the white rectangular in (b) corresponds to a defocus of -5 nm and a sample thickness of 7 nm [1]. A projection of the crystal structure onto the *bc* plane is overlaid on the HAADF-STEM image shown in (b). Red, yellow, green and light blue spheres indicate Sr(1), Sr(2), Mn/Sb(1) and Mn(2) atoms, respectively. An average background subtraction filter has been applied to image (b) to remove contributions from an amorphous layer [2].

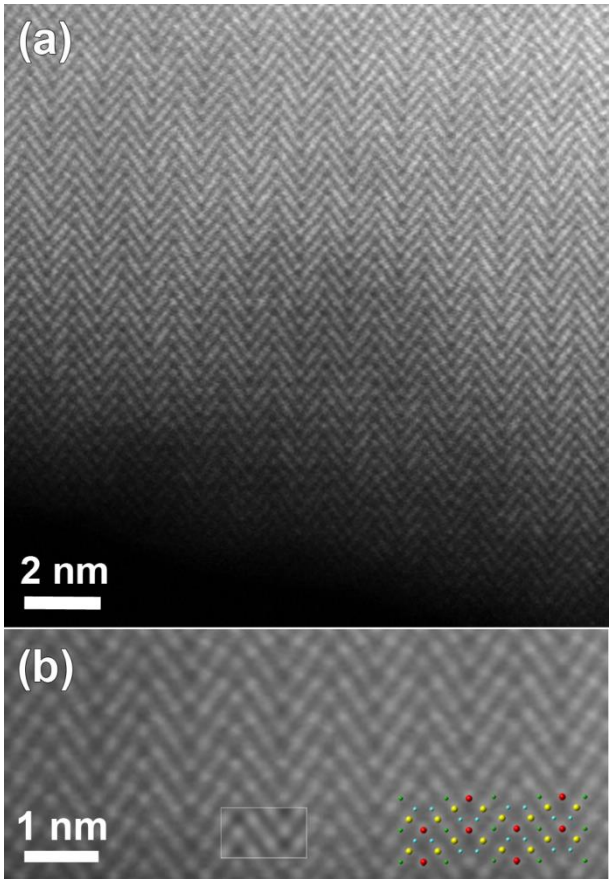

[1] P.A. Stadelmann, jEMS- A program for the simulation of images and diffraction patterns in electron microscope, 2007, EPFL, Lausanne.

[2] R. Kilaas, *Journal of Microscopy*, 1998, **190**, 45.

Table S1. Structural data for $SrMn_{1-x}Sb_xO_3$ (x = 0.025 - 0.415) obtained from XRPD data

	x = 0.025	x = 0.05	x = 0.075	x = 0.10	x = 0.125	x = 0.165	x = 0.20	x = 0.25	x = 0.335	x = 0.415
Formula	$SrMn_{0.975}Sb_{0.025}O_3$	$SrMn_{0.95}Sb_{0.05}O_3$	$SrMn_{0.925}Sb_{0.075}O_3$	$SrMn_{0.90}Sb_{0.10}O_3$	$SrMn_{0.875}Sb_{0.125}O_3$	$SrMn_{0.835}Sb_{0.165}O_3$	$SrMn_{0.80}Sb_{0.20}O_3$	$SrMn_{0.75}Sb_{0.25}O_3$	$SrMn_{0.665}Sb_{0.335}O_3$	$SrMn_{0.585}Sb_{0.415}O_3$
Mass % Monoclinic	**95.4[a]**	**100.0**	**100.0**	**93.6**	**69.9**	**39.2**				
Space group, #	*C2/c*, 15	*C2/c*, 15	*C2/c*, 15	*C2/c*, 15	*C2/c*, 15	*C2/c*, 15				
Z	12	12	12	12	12	12				
Cell constants:										
a, Å	5.4397(2)	5..4510(2)	5.46832(8)	5.4733(1)	5.4746(2)	5.4779(5)				
b, Å	9.4200(3)	9.4378(3)	9.4631(1)	9.4738(2)	9.4721(3)	9.4735(8)				
c, Å	13.4411(5)	13.4747(4)	13.5131(3)	13.5361(3)	13.5295(5)	13.521(2)				
β, °	90.595(2)	90.586(2)	90.655(1)	90.692(1)	90.697(2)	90.744(7)				
V, $Å^3$	688.71(4)	693.17(3)	699.22(2)	701.83(2)	701.53(4)	701.61(1)				
Mass % Tetragonal				**6.4**	**30.1**	**60.8**	**100.0**	**100.0**	**100.0**	**100.0**
Space group, #				*I4/mcm*, 140	*I4/mcm*, 140	*I4/mcm*, 140	*I4/mcm*, 140	*I4/mcm*, 140	*I4/mcm*, 140	*I4/mcm*, 140
Z				4	4	4	4	4	4	4
Cell constants:										
a=b, Å				5.4314(2)	5.4265(1)	5.42309(8)	5.42903(5)	5.43903(5)	5.46888(5)	5.49081(3)
c, Å				7.8307(6)	7.8325(2)	7.8395(1)	7.87111(10)	7.9234(12)	8.0172(1)	8.04552(5)
V, $Å^3$				231.01(2)	230.644(9)	230.559(7)	231.996(4)	234.399(5)	239.783(7)	242.564(3)
wRp/ Rp, %	2.25/1.37	2.27/1.47	1.15/0.86	1.53/1.05	1.71/1.22	2.47/1.62	2.92/1.88	3.15/1.92	3.89/2.48	2.80/1.92
CHI^2	7.951	3.771	2.008	3.307	2.851	3.708	4.438	7.472	5.168	3.282
$R(F^2)$	7.24	5.88	3.82	4.25	5.23	6.08	2.92	2.76	2.50	2.06

[a] This sample contains impurities of 2.0 mass % of $SrMnO_3$ and 2.6 mass % of $Sr_4Mn_3O_{10}$

Table S2. Selected interatomic distances d (Å), oxidation state of manganese and bond valence sums for the $SrMn_{1-x}Sb_xO_3$ (x = 0.075, 0.20, 0.335, 0.415) at room temperature

x = 0.15, $Mn^{+3.92}$=0.92 Mn^{+4}+0.08 Mn^{+3}					
Interatomic distances		Interatomic distances		Interatomic distances	
Sr(1)-O(1) ×2	2.7371(4)	Sr(2)-O(1)	2.734(6)	Mn/Sb(1)-O(3) ×2	1.923(6)
Sr(1)-O(2) ×2	2.707(8)	Sr(2)-O(2)	2.654(5)	Mn/Sb(1)-O(4) ×2	1.947(5)
Sr(1)-O(2) ×2	2.767(9)	Sr(2)-O(2)	2.847(5)	Mn/Sb(1)-O(5) ×2	1.920(5)
Sr(1)-O(3) ×2	2.747(8)	Sr(2)-O(3)	2.840(7)	**Mn/Sb(1)-O**	**1.930**
Sr(1)-O(4) ×2	2.928(6)	Sr(2)-O(3)	2.617(8)	Expected[a]	1.949
Sr(1)-O(5) ×2	2.622(6)	Sr(2)-O(3)	2.856(8)	BVS Mn^{+4}	3.722
Sr(1)-O	**2.751**	Sr(2)-O(4)	2.775(9)	BVS Sb^{+5}	6.202
Expected[a]	2.84	Sr(2)-O(4)	2.711(9)		
BVS	2.232	Sr(2)-O(4)	2.675(6)	Mn(2)-O(1)	1.946(8)
		Sr(2)-O(5)	2.710(10)	Mn(2)-O(2)	1.877(5)
Mn(2)-Mn(2)	2.508(3)	Sr(2)-O(5)	2.757(10)	Mn(2)-O(2)	1.927(6)
		Sr(2)-O(5)	2.958(6)	Mn(2)-O(3)	1.870(8)
BVS O(1)	1.942	**Sr(2)-O**	**2.761**	Mn(2)-O(4)	1.880(6)
BVS O(2)	2.091	Expected[a]	2.84	Mn(2)-O(5)	1.904(6)
BVS O(3)	2.177	BVS	2.176	**Mn(2)-O**	**1.901**
BVS O(4)	2.094			Expected[a]	1.934
BVS O(5)	2.136			BVS	4.037

x = 0.40, $Mn^{+3.75}$ =0.75 Mn^{+4}+0.25 Mn^{+3}		x = 0.67, $Mn^{+3.5}$ =0.5 Mn^{+4}+0.5 Mn^{+3}		x = 0.83, $Mn^{+3.29}$ =0.29 Mn^{+4}+0.71 Mn^{+3}	
Interatomic distances		Interatomic distances		Interatomic distances	
Sr-O(1) ×4	2.71429(2)	Sr-O(1) ×4	2.73444(3)	Sr-O(1) ×4	2.74520(1)
Sr-O(2) ×4	2.8472(10)	Sr-O(2) ×4	2.9286(15)	Sr-O(2) ×4	2.9566(7)
Sr-O(2) ×4	2.6538(9)	Sr-O(2) ×4	2.6488(13)	Sr-O(2) ×4	2.6433(6)
Sr-O	**2.738**	**Sr-O**	**2.771**	**Sr-O**	**2.782**
Expected[a]	2.84	Expected[a]	2.84	Expected[a]	2.84
BVS	2.296	BVS	2.156	BVS	2.12
Mn/Sb-O(1) ×2	1.96772(2)	Mn/Sb-O(1) ×2	2.00430(2)	Mn/Sb-O(1) ×2	2.01126(1)
Mn/Sb-O(2) ×4	1.92426(10)	Mn/Sb-O(2) ×4	1.94405(21)	Mn/Sb-O(2) ×4	1.95425(11)
Mn/Sb-O	**1.939**	**Mn/Sb-O**	**1.964**	**Mn/Sb-O**	**1.973**
Expected[a]	1.954	Expected[a]	1.970	Expected[a]	1.980
BVS Mn^{+3}	3.708	BVS Mn^{+3}	3.466	BVS Mn^{+3}	3.382
BVS Mn^{+4}	3.638	BVS Mn^{+4}	3.402	BVS Mn^{+4}	3.32
BVS Sb^{+5}	6.064	BVS Sb^{+5}	5.672	BVS Sb^{+5}	5.532
BVS O(1)	2.067	BVS O(1)	2.002	BVS O(1)	2.013
BVS O(2)	2.176	BVS O(2)	2.166	BVS O(2)	2.182

[a] The sum of the crystal radii according to [R. D. Shannon, "Revised effective ionic radii and systematic studies of interatomic distances in halides and chalcogenides," Acta Crystallographica A, vol. 32, no. 5, pp. 751–767, 1976]: Sr^{+2} XII – 1.58 Å, Sb^{+5} VI - 0.74 Å, Mn^{+3} VI LS- 0.72 Å, Mn^{+4} VI - 0.67 Å, O^{-2} VI – 1.26 Å. For Mn/Sb sites expected distances are calculated taking in account fractions of manganese and antimony.

[b] The average values are indicated by boldface type.

Table S3. Structural data for $SrMn_{1-x}Sb_xO_3$ for x = 0.075

		T=1.5 K NPD	T=80 K NPD	T=298 K XRPD+NPD	T=500 K NPD
Space group, #, *Z*		*C2/c*, 15, 12	*C2/c*, 15, 12	*C2/c*, 15, 12	*C2/c*, 15, 12
Cell constants:					
a, Å		5.4602(2)	5.4612(2)	5.46826(7)	5.4829(3)
b, Å		9.4339(2)	9.4353(2)	9.4629(1)	9.4902(5)
c, Å		13.4951(4)	13.4971(4)	13.5140(2)	13.5423(6)
β, °		90.773(2)	90.764(2)	90.6545(9)	90.555(3)
V, Å^3		695.08(4)	695.42(3)	699.24(2)	704.64(6)
Sr(1) - 4*e* (0, *y*, 1/4)	*y*	-0.0025(8)	-0.0009(9)	-0.0015(4)	0.0027(17)
	U_i/U_e*100	1.46(9)	1.4(1)	1.11(7)	2.34(13)
Sr(2) - 8*f* (*x*, *y*, *z*)	*x*	0.0071(7)	0.0063(7)	0.0056(3)	0.0049(10)
	y	0.3324(7)	0.3333(7)	0.3334(4)	0.3341(12)
	z	0.0900(3)	0.0902(3)	0.09109(9)	0.0903(3)
	U_i/U_e*100	1.71(8)	1.67(7)	1.26(5)	2.65(10)
Mn/Sb(1) - 4*a* (0, 0, 0)	U_i/U_e*100	1.20(6)[b]	1.16(6)[b]	0.66(9)	1.71(9)[b]
	Fraction	0.775/0.225	0.775/0.225	0.775/0.225	0.775/0.225
Mn(2) - 8*f* (*x*, *y*, *z*)	*x*	0.9905(9)	0.9905(9)	-0.0060(4)	-0.0040(10)
	y	0.3334(11)	0.3345(11)	0.3307(6)	0.3290(18)
	z	0.8422(3)	0.8429(3)	0.8427(1)	0.8426(4)
	U_i/U_e*100	1.20(7)[b]	1.16(6)[b]	1.55(7)	1.71(9)[b]
O(1) - 4*e* (0, *y*, 1/4)	*y*	0.5140(8)	0.5125(9)	0.5121(8)	0.5145(19)
	U_i/U_e*100	1.7(2)	1.7(2)	0.6(2)	2.2(4)
O(2) - 8*f* (*x*, *y*, *z*)	*x*	0.2691(11)	0.2688(11)	0.2680(12)	0.2687(20)
	y	0.2428(6)	0.2420(6)	0.2387(6)	0.2413(9)
	z	0.2436(4)	0.2436(4)	0.2437(4)	0.2468(5)
	U_i/U_e*100	1.7(1)	1.7(1)	1.7(1)	2.2(2)
O(3) - 8*f* (*x*, *y*, *z*)	*x*	0.0303(14)	0.0298(14)	0.0272(15)	0.0146(33)
	y	0.8340(7)	0.8348(7)	0.8350(7)	0.8347(11)
	z	0.0824(5)	0.0821(5)	0.0825(5)	0.0819(9)
	U_i/U_e*100	2.1(2)	2.0(2)	1.0(2)	2.7(3)
O(4) - 8*f* (*x*, *y*, *z*)	*x*	0.2719(9)	0.2731(10)	0.2702(12)	0.2603(24)
	y	0.0833(7)	0.0836(7)	0.0844(8)	0.0841(15)
	z	0.0716(3)	0.0718(4)	0.0742(4)	0.0761(7)
	U_i/U_e*100	1.7(1)	1.8(1)	1.5(1)	3.1(2)
O(5) - 8*f* (*x*, *y*, *z*)	*x*	0.7761(11)	0.7768(11)	0.7688(14)	0.7690(21)
	y	0.0834(8)	0.0832(8)	0.0818(8)	0.0835(14)
	z	0.0913(4)	0.0916(4)	0.0893(4)	0.0886(6)
	U_i/U_e*100	1.4(1)	1.4(1)	1.5(2)	2.6(2)
wRp, X-ray/Neutron, %		-/4.46 -/4.72[a]	-/4.45 -/4.55[a]	1.15/4.53	-/4.33
Rp, X-ray/Neutron, %		-/3.41 -/3.60[a]	-/3.39 -/3.46[a]	0.84/3.54	-/3.43
χ^2		-/1.698 -/1.916[a]	-/1.691 -/1.783[a]	1.925	1.579
R(F^2), X-ray/Neutron, %		-/2.20 -/2.43[a]	-/2.31 -/2.41[a]	2.75/2.92	-/2.76
Thermal expansion:					
a_a, $10^{-6}K^{-1}$			2.333	5.922	13.218
a_b, $10^{-6}K^{-1}$			1.890	13.379	14.241
a_c, $10^{-6}K^{-1}$			1.888	5.737	10.345
a_V, $10^{-6}K^{-1}$			6.228	25.060	37.938

[a] R-factors obtained without taking into account the magnetic ordering.

[b] Thermal parameters of Mn/Sb(1) and Mn(2) atoms were constrained as single variable.

Table S4. Structural data for $SrMn_{1-x}Sb_xO_3$ for x = 0.20, 0.335 and 0.415

	T = 5 K (NPD)		T = 298 K (XRPD+NPD)			T = 500 K (NPD)	
	0.20	0.335	0.20	0.335	0.415	0.20	0.335
Space group, #, *Z*	*I4/mcm*, 140, 4	*I4/mcm*, 140, 4	*I4/mcm*, 140, 4	*I4/mcm*, 140, 4	*I4/mcm*, 140, 4	$Pm\overline{3}m$, 221, 1	*I4/mcm*, 140, 4
Cell constants:							
a=*b*, Å	5.40299(3)	5.4518(1)	5.42858(3)	5.46888(5)	5.49039(3)	3.87998(2)	5.5065(1)
c, Å	7.8967(1)	8.0571(4)	7.87086(8)	8.0172(1)	8.04503(5)		7.9727(2)
V, $Å^3$	230.522(3)	239.47(2)	231.950(3)	239.783(7)	242.513(2)	58.4101(6)	241.742(9)
Sr(1)	4*b*	4*b*	4*b*	4*b*	4*b*	1*b*	4*b*
x, *y*, *z*	(0, 1/2, 1/4)	(0, 1/2, 1/4)	(0, 1/2, 1/4)	(0, 1/2, 1/4)	(0, 1/2, 1/4)	(1/2, 1/2, 1/2)	(0, 1/2, 1/4)
U_i/U_e*100	0.91[a]	1.04[a]	1.99[a]	2.24[a]	2.33[a]	1.74[a]	2.19[a]
Mn/Sb(1)	4*c*	4*c*	4*c*	4*c*	4*c*	1*a*	4*c*
x, *y*, *z*	(0, 0, 0)	(0, 0, 0)	(0, 0, 0)	(0, 0, 0)	(0, 0, 0)	(0, 0, 0)	(0, 0, 0)
U_i/U_e*100	1.2(1)	2.50[a]	1.82[a]	1.87[a]	2.23(3)	1.60[a]	2.50[a]
Fraction	0.8/0.2	0.667/0.333	0.8/0.2	0.667/0.333	0.585/0.415	0.8/0.2	0.667/0.333
O(1)	4*a*	4*a*	4*a*	4*a*	4*a*	3*d*	4*a*
x, *y*, *z*	(0, 0, 1/4)	(0, 0, 1/4)	(0, 0, 1/4)	(0, 0, 1/4)	(0, 0, 1/4)	(1/2, 0, 0)	(0, 0, 1/4)
U_i/U_e*100	0.86[a]	1.35[a]	1.85[a]	2.07[a]	2.35[a]	1.92[a]	2.25[a]
O(2)	8*h*	8*h*	8*h*	8*h*	8*h*		8*h*
x, *y*, *z*	(*x*, *x*+1/2, 0)	(*x*, *x*+1/2, 0)	(*x*, *x*+1/2, 0)	(*x*, *x*+1/2, 0)	(*x*, *x*+1/2, 0)		(*x*, *x*+1/2, 0)
x	0.2738(2)	0.2815(2)	0.2681(2)	0.2761(3)	0.2791(3)		0.2693(3)
U_i/U_e*100	0.99[a]	1.13[a]	1.69[a]	1.74[a]	2.20[a]		2.16[a]
wRp, X-ray/Neutron, %	-/5.26	-/5.06	2.82/5.54	3.83/4.77	2.68/4.49	-/4.70	-/5.06
Rp, X-ray/Neutron, %	-/4.07	-/3.86	1.80/4.25	2.39/3.74	1.84/3.50	-/3.67	-/3.89
χ^2	2.249	2.070	3.637	4.213	2.605	1.784	2.016
$R(F^2)$, X-ray/Neutron, %	-/3.64	-/3.19	2.26/3.20	1.72/3.07	1.22/2.02	-/1.86	-/3.15
Thermal expansion:							
a_a, $10^{-6}K^{-1}$			16.089	10.659		52.815	33.821
a_c, $10^{-6}K^{-1}$			-11.205	-16.986		-70.749	-27.631
a_V, $10^{-6}K^{-1}$			21.012	4.455		35.817	40.551

[a] U_{eqv}*100 calculated from anisotropic thermal factors defined by $T = e\,[-2\pi^2(u_{11}h^2a^{*2} + \ldots + 2u_{12}hka^*b^* + \ldots)]$

Table S5. Irreducible representation of Gk for space group *C*2/*c* and k=(0,0,0) with p=1/2.

IRREPs	Symmetry operators			
	{1|000}	{2_0y0|00p}	{-1|000}	{m_x0z|00p}
Γ_1	1	1	1	1
Γ_2	1	1	-1	-1
Γ_3	1	-1	1	-1
Γ_4	1	-1	-1	1

Table S6. The general expressions of the Fourier coefficients Sk(j) of the atoms non-related by lattice translations for sites 4*a* and 8*f* in space group *C*2/*c*.

	Γ_1	Γ_2	Γ_3	Γ_4	Atom	Symmetry
Site 4*a*						
Sk(1)	(u, v, w)		(u, v, w)		Mn11	0, 0, 0
Sk(2)	(-u, v, -w)		(u,-v,w)		Mn12	0, 0, 1/2
Site 8*f*						
Sk(1)	(u, v, w)	(u, v, w)	(u, v, w)	(u, v, w)	Mn21	x, y, z
Sk(2)	(-u, v, -w)	(-u, v, -w)	(u, -v, w)	(u, -v, w)	Mn22	-x+1, y, -z+3/2
Sk(3)	(u, v, w)	(-u, -v, -w)	(u, v, w)	(-u, -v, -w)	Mn23	-x+1, -y+1, -z+1
Sk(4)	(-u, v, -w)	(u, -v, w)	(u, -v, w)	(-u, v, -w)	Mn28	x-1/2, -y+1/2, z-1/2

Table S7. The general expressions of the Fourier coefficients Sk(j) of the atoms non-related by lattice translations for sites 2*a* and 4*f* in space group *P*6$_3$/*mmc*.

	Γ_2	Γ_3	Γ_5	Γ_6	Γ_8	Γ_9	Γ_{11}	Γ_{12}	Atom	Symmetry
Site 2*a*										
Sk(1)		(0, 0, u)		$m_z=0^a$		(0, 0, u)		$m_z=0^a$	Mn11	0, 0, 0
Sk(2)		(0, 0, u)		$m_z=0^a$		(0, 0, -u)		$m_z=0^a$	Mn12	0, 0, 1/2
Site 4*f*										
Sk(1)	(0, 0, u)	(0, 0, u)	$m_z=0^a$	$m_z=0^a$	(0, 0, u)	(0, 0, u)	$m_z=0^a$	$m_z=0^a$	Mn21	x, y, z
Sk(2)	(0, 0, u)	(0, 0, u)	$m_z=0^a$	$m_z=0^a$	(0, 0, -u)	(0, 0, -u)	$m_z=0^a$	$m_z=0^a$	Mn24	-x+1, -y+1, z-1/2
Sk(3)	(0, 0, -u	(0, 0, u	$m_z=0^a$	$m_z=0^a$	(0, 0, -u	(0, 0, u	$m_z=0^a$	$m_z=0^a$	Mn23	y, x, -z+1
Sk(4)	(0, 0, -u)	(0, 0, u)	$m_z=0^a$	$m_z=0^a$	(0, 0, u)	(0, 0, -u)	$m_z=0^a$	$m_z=0^a$	Mn22	-y+1, -x+1, -z+3/2

[a] Fourier coefficients of type: r0.(u,-v,0)+i.(-u+2v,-2u+v,0), where $m_z=0$.

Table S8. Magnetic Moments at 1.5 K and 80 K (given in Italic) for Mn^{4+} in $SrMn_{0.925}Sb_{0.075}O_3$ in Cartesian Coordinates

Name	*x*	*y*	*z*	*Mx*/μ_B		*My*/μ_B		*Mz*/μ_B		*M*/μ_B		Fraction
Mn11	0	0	0	0	*0*	0	*0*	1.85(9)	*1.4(1)*	1.85(9)	*1.4(1)*	0.775
Mn12	0	0	0.5	0	*0*	0	*0*	-1.85(9)	*-1.4(1)*	1.85(9)	*1.4(1)*	0.775
Mn13	0.5	0.5	0	0	*0*	0	*0*	1.85(9)	*1.4(1)*	1.85(9)	*1.4(1)*	0.775
Mn14	0.5	0.5	0.5	0	*0*	0	*0*	-1.85(9)	*-1.4(1)*	1.85(9)	*1.4(1)*	0.775
Mn21	0.9905(9)	0.3334(11)	0.8422(4)	0	*0*	0	*0*	-1.13(6)	*-0.91(8)*	1.13(6)	*0.91(8)*	1.0
Mn22	0.0095(9)	0.3334(11)	0.6578(4)	0	*0*	0	*0*	1.13(6)	*0.91(8)*	1.13(6)	*0.91(8)*	1.0
Mn23	0.0095(9)	0.6666(11)	0.1578(4)	0	*0*	0	*0*	-1.13(6)	*-0.91(8)*	1.13(6)	*0.91(8*	1.0
Mn24	0.9905(9)	0.6666(11)	0.3422(4)	0	*0*	0	*0*	1.13(6)	*0.91(8)*	1.13(6)	*0.91(8*	1.0
Mn25	0.4905(9)	0.8334(11)	0.8422(4)	0	*0*	0	*0*	-1.13(6)	*-0.91(8)*	1.13(6)	*0.91(8*	1.0
Mn26	0.5095(9)	0.8334(11)	0.6578(4)	0	*0*	0	*0*	1.13(6)	*0.91(8)*	1.13(6)	*0.91(8*	1.0
Mn27	0.5095(9)	0.1666(11)	0.1578(4)	0	*0*	0	*0*	-1.13(6)	*-0.91(8)*	1.13(6)	*0.91(8*	1.0
Mn28	0.4905(9)	0.1666(11)	0.3422(4)	0	*0*	0	*0*	1.13(6)	*0.91(8)*	1.13(6)	*0.91(8*	1.0

Table S9. The general expressions of the Fourier coefficients Sk(j) of the atoms non-related by lattice translations for sites 4*c* in space group *I*4/*mcm*.

	Γ_1	Γ_7	Γ_{10}	Atom	Symmetry
Sk(1)	(0, 0, u)	(0, 0, u)	(u+p, v-w, 0)	Mn1	0, 0, 0
Sk(2)	(0, 0, -u)	(0, 0, u)	(-u+p, v+w, 0)	Mn2	0, 0, 1/2

Table S10. Magnetic Moments at 5 K for Mn^{4+} in $SrMn_{0.80}Sb_{0.20}O_3$ and $SrMn_{0.665}Sb_{0.335}O_3$ (given in Italic) in Cartesian Coordinates

Name	*x*	*y*	*z*	*Mx*/μ_B		*My*/μ_B		*Mz*/μ_B		*M*/μ_B		Fraction	
Mn1	0	0	0	0	*0*	0	*0*	2.79(2)	*2.00(4)*	2.79(2)	*2.00(4)*	*0.8*	0.667
Mn2	0	0	0.5	0	*0*	0	*0*	2.79(2)	*2.00(4)*	2.79(2)	*2.00(4)*	*0.8*	0.667
Mn3	0.5	0.5	0	0	*0*	0	*0*	-2.79(2)	*-2.00(4)*	2.79(2)	*2.00(4)*	*0.8*	0.667
Mn4	0.5	0.5	0.5	0	*0*	0	*0*	-2.79(2)	*-2.00(4)*	2.79(2)	*2.00(4)*	*0.8*	0.667

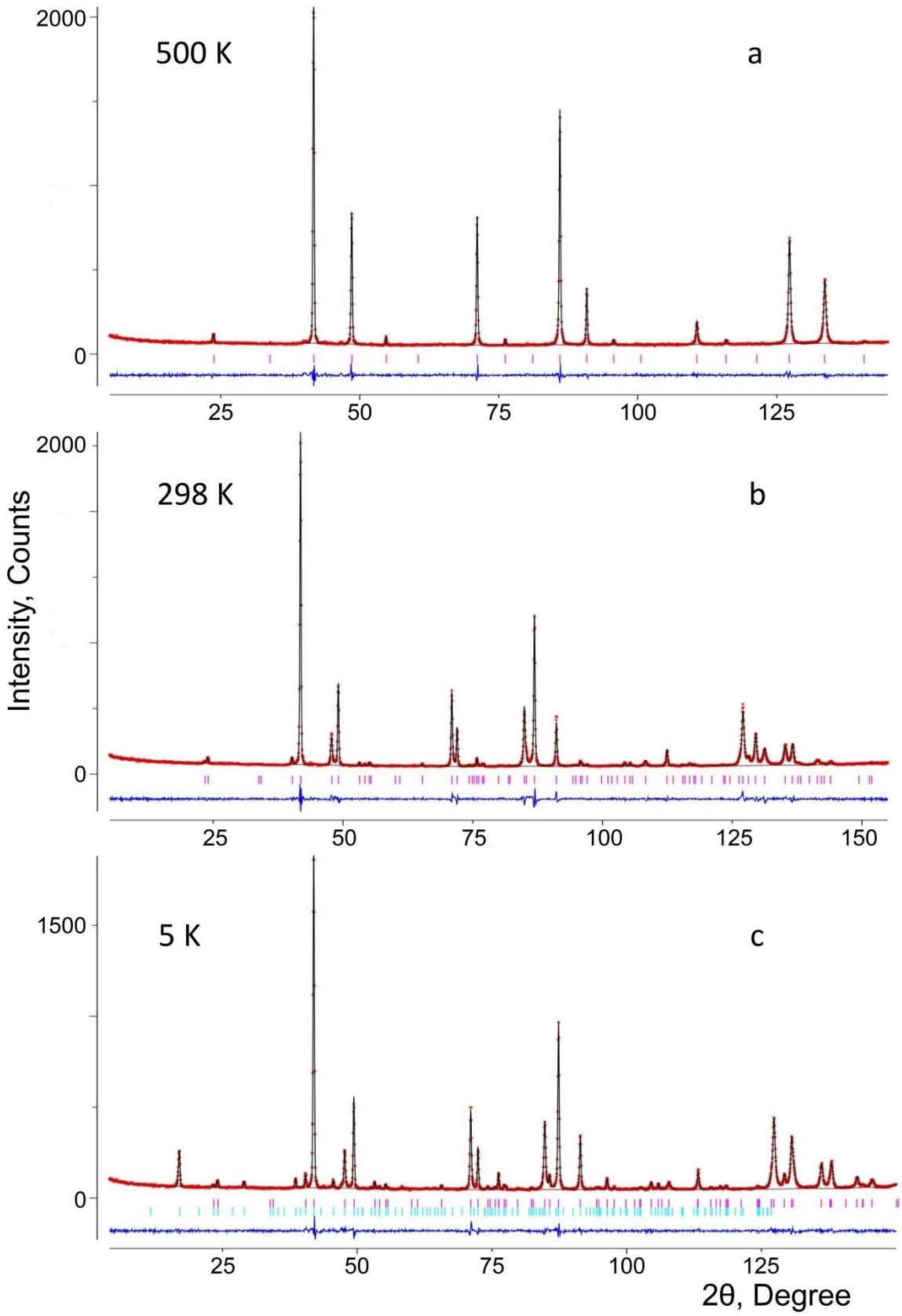

Figure S2. Neutron diffraction pattern of $SrMn_{0.8}Sb_{0.2}O_3$ at 500 K (a), 298 K (b) and 5 K (c). The red crosses are experimental points, the solid black line is the calculated profile, and the vertical marks correspond to the positions of the Bragg reflections for the crystallographic (purple, first row) and magnetic (blue, second row) structures. The difference curve is plotted at the bottom of the figure.